21st International Symposium on
Mathematical Theory of Networks and Systems
July 7-11, 2014. Groningen, The Netherlands

Inversion-based feedforward control for discretized port-Hamiltonian systems

Paul Kotyczka, Sebastian Brandstäter[1]

Abstract— **The paper deals with the feedforward control problem for a class of hyperbolic distributed parameter systems in one spatial dimension (generalized transmission systems). Based on the models obtained from a structure preserving port-Hamiltonian discretization, a modular approach is presented to determine input trajectories which correspond to prespecified trajectories of the non-collocated outputs. The presence of a feedthrough term in the discretized models allows to immediately express the inverse dynamics which must be integrated to solve the feedforward control problem. In general, the inverse dynamics for non-collocated pairs of in- and outputs is unstable, hence, techniques from the dynamic inversion of non-minimum phase systems can be applied. The resulting modular approach is presented for linear systems, and, as a sketch, for the nonlinear case. The proposed procedure is a building block to solve the feedforward control problem in networks of nonlinear transmission systems.**

I. INTRODUCTION

The class of systems considered in this paper arises from the structure preserving discretization of hyperbolic port-Hamiltonian distributed-parameter systems with the method introduced in [1]. Typical nonlinear examples, which, due to their structural similarity to electric transmission lines, can be understood as generalized transmission systems, are fluid flows e. g. in pipelines or open channels [2], [3]. An advantage of port-Hamiltonian modeling and structure preserving discretization is that nonlinear transmission systems (the nonlinearity resulting from a non-quadratic energy functional) are naturally included in the approach.

With the common choice of one-forms and shape functions to approximate the spatial distributions of the state and effort variables, the finite-dimensional discretized state representation of each segment has a port-Hamiltonian structure containing a feedthrough term. The interconnection, damping and input matrices for single transmission lines as well as for a transmission network can be constructed in a recursive way from the basic model of one segment [4].

The resulting discretized models have relative degree zero, which on the one hand is in opposition to the physical nature of transmission systems. (Yet, the discretized models approximate the typical transmission delays in the simulation.) On the other hand, the feedthrough term helps to reformulate the equations and to reassign the roles of in- and outputs. In this paper, the non-collocated case is focussed, where inputs and outputs are situated at opposite terminals of the system. The differential equation for the *inverse dynamics*, as discussed for the purpose of feedforward control, is excited by the desired outputs (boundary efforts / conjugated power variables at one terminal of the system). The control inputs at the opposite terminal are obtained from the output equation of the inverse system. The inverse dynamics of the considered models with zero relative degree can be understood as the full order internal dynamics.

It will be shown that in general (except in strongly damped cases), the inverse dynamics is unstable, which impedes to determine the feedforward control input by a simple (forward in time) integration of the inverse system. Then the problem at hand is the dynamic inversion of a non-minimum phase system whose solution – if not an optimization based technique is employed like described in [5] – involves integrations forward and backward in time along the stable and unstable manifolds of the inverse/internal dynamics [6].

The remainder of the paper is organized as follows. In Section II the models under consideration are introduced. The class of distributed-parameter transmission systems in one spatial dimension is described, as well as the structure preserving discretization procedure and the structure of the resulting finite-dimenstional models. In Section III the model properties are discussed and a stability condition for the non-collocated inverse dynamics is presented. Section IV addresses the feedforward control problem to track the non-collocated outputs. It is shown at the linear case how the modularity of the discretized models can be exploited to compute feedforward controllers in an iterative manner. An extension to the nonlinear case is sketched and the difficulties to be solved in this setting are discussed. Section V shows how the procedure can be applied to generate transient input trajectories for set point changes in the operation of nonlinear transmission networks, as a generalization of the approach proposed in [7] for linear HVDC networks. Open questions and future research directions are formulated in the conclusions Section VI.

II. MODELS FROM STRUCTURE PRESERVING DISCRETIZATION

A. Class of infinite-dimensional systems

The considered class of distributed parameter systems in one spatial dimension z comprises transmission systems like electrical transmission lines or fluidic pipeline or channel systems. The dynamics of these systems is governed by two scalar (quasi-)linear partial differential equations of hyperbolic type and can be expressed in a unified manner

[1]The authors are with the Institute of Automatic Control, Technische Universität München (Prof. Boris Lohmann), Boltzmannstr. 15, 85748 Garching, Germany {kotyczka, sebastian.brandstaeter}@tum.de

ISBN: 978-90-367-6321-9

in port-Hamiltonian form by

$$\partial_t \boldsymbol{\alpha}(z,t) = \boldsymbol{P}_1 \partial_z \boldsymbol{\beta}(z,t) - \boldsymbol{R}_0 \boldsymbol{\beta}(z,t). \tag{1}$$

The greek letters[1] denote the 2-dimensional vectors of distributed states $\boldsymbol{\alpha}(z,t)$ and co-states or effort variables $\boldsymbol{\beta}(z,t)$, whose elements, in contrast to the lumped-parameter case, are functions of time t and the spatial variable $z \in [0, L]$ on the considered interval. The matrices

$$\boldsymbol{P}_1 = \begin{bmatrix} 0 & -1 \\ -1 & 0 \end{bmatrix}, \quad \boldsymbol{R}_0 = \begin{bmatrix} \rho_1 & 0 \\ 0 & \rho_2 \end{bmatrix} \tag{2}$$

with $\rho_1, \rho_2 \geq 0$, stand for energy exchange and dissipation, as in the lumped-parameter case. The distributed effort variables $\boldsymbol{\beta}(z,t)$ can be derived from the energy functional

$$h(\boldsymbol{\alpha}) = \int_0^L \mathcal{H}(\boldsymbol{\alpha}(z,t))\, dz, \tag{3}$$

where $\mathcal{H}(\boldsymbol{\alpha}(z,t))$ denotes the Hamiltonian (or energy) density, according to

$$\boldsymbol{\beta}^T(z,t) = \delta_\alpha h(\boldsymbol{\alpha}(z,t)). \tag{4}$$

$\delta_\alpha h$ denotes the (row) vector of variational derivatives of h, defined according to

$$h(\boldsymbol{\alpha} + \varepsilon \boldsymbol{\eta}) = h(\boldsymbol{\alpha}) + \varepsilon \int_0^L \delta_\alpha h\, \boldsymbol{\eta}\, dz + \mathcal{O}(\varepsilon^2), \tag{5}$$

where $\varepsilon > 0$ is small and the variation $\boldsymbol{\eta}(z,t)$ is chosen such that $\boldsymbol{\alpha}(z,t) + \varepsilon \boldsymbol{\eta}(z,t)$ satisfies the same boundary conditions as $\boldsymbol{\alpha}(z,t)$. The boundary efforts $\boldsymbol{\beta}(0,t)$, $\boldsymbol{\beta}(L,t)$ will be assigned as in- and outputs of the (discretized) models, depending on their role. Substituting $\varepsilon = dt$, $\boldsymbol{\eta}(z,t) = \dot{\boldsymbol{\beta}}(z,t)$ in (5), the time derivative of $h(\boldsymbol{\alpha})$ can be formulated, which yields the energy balance equation

$$\begin{aligned} \dot{h} = \int_0^L \delta_\alpha h\, \dot{\boldsymbol{\alpha}}\, dz = \int_0^L \boldsymbol{\beta}^T \boldsymbol{P}_1 \partial_z \boldsymbol{\beta}\, dz - \int_0^L \boldsymbol{\beta}^T \boldsymbol{R}_0 \boldsymbol{\beta}\, dz \leq \\ \leq \beta_1(0)\beta_2(0) - \beta_1(L)\beta_2(L). \end{aligned} \tag{6}$$

For further details, the reader is referred to [8].

B. Discretization procedure

As described in [1], the distributed states and efforts on one segment with $z \in [a,b]$, $0 \leq a < b \leq L$ are approximated by a separation of spatial shape functions $\omega_i^{ab}(z)$ and $\omega_i^{a/b}(z)$ and time-dependent states $x_i(t)$ and boundary efforts and $e_i^{a/b}(t)$ of the discretized model ($i = 1, 2$):

$$\alpha_i(z,t) \approx \omega_i^{ab}(z) x_i(t), \tag{7}$$

$$\beta_i(z,t) \approx \omega_i^a(z) e_i^a(t) + \omega_i^b(z) e_i^b(t). \tag{8}$$

The states of the discretized model are supposed to approximate the integral of the distributed states, while the boundary efforts should match the corresponding values in the distributed parameter model:

$$x_i(t) \approx \int_a^b \alpha_i(z,t)\, dz \tag{9}$$

$$e_i^a(t) \approx \beta_i(a,t), \qquad e_i^b(t) \approx \beta_i(b,t). \tag{10}$$

These requirements translate into the conditions

$$\int_a^b \omega_i^{ab}(z)\, dz = 1, \tag{11}$$

$$\begin{aligned} \omega_i^a(a) = 1, \quad \omega_i^a(b) = 0, \\ \omega_i^b(a) = 0, \quad \omega_i^b(b) = 1, \end{aligned} \tag{12}$$

where it becomes apparent that $\omega_i^{ab}(z)$ can be understood as a 1-form, wheras $\omega_i^{a/b}(z)$ are 0-forms (functions).

Replacing (7) and (8) in the partial differential equations (1), where for the moment the dissipation is ignored, i. e. $\rho_1 = \rho_2 = 0$ is assumed, yields

$$\begin{aligned} \omega_1^{ab}(z)\dot{x}_1(t) &= -\left(\partial_z \omega_2^a(z) e_2^a(t) + \partial_z \omega_2^b(z) e_2^b(t)\right) \\ \omega_2^{ab}(z)\dot{x}_2(t) &= -\left(\partial_z \omega_1^a(z) e_1^a(t) + \partial_z \omega_1^b(z) e_1^b(t)\right). \end{aligned} \tag{13}$$

The simplest possible choice of shape functions such that the terms depending on z cancel in (13) is ($i = 1, 2$)

$$\omega_i^{ab} = \frac{1}{b-a}, \qquad \omega_i^a(z) = \frac{b-z}{b-a}, \quad \omega_i^b(z) = \frac{z-a}{b-a}. \tag{14}$$

What remains is the set of two ordinary differential equations, excited by the boundary efforts[2]

$$\begin{aligned} \dot{x}_1 &= e_2^a - e_2^b \\ \dot{x}_2 &= e_1^a - e_1^b. \end{aligned} \tag{15}$$

In a next step, the average effort variables on one segment

$$e_i = \frac{1}{2}(e_i^a + e_i^b) \tag{16}$$

are defined. It can be verified that indeed they can be expressed as partial derivatives of the approximate energy on the interval $[a,b]$, with $\Delta = b - a$,

$$\boldsymbol{e} = \nabla H^{ab}(\boldsymbol{x}), \quad H^{ab}(\boldsymbol{x}) = \Delta \mathcal{H}(\frac{\boldsymbol{x}}{\Delta}) \approx \int_a^b \mathcal{H}(\boldsymbol{\alpha}(z)) dz. \tag{17}$$

One choice of inputs and collocated outputs such that $y_i u_i$, $i = 1, 2$ is the power supplied to the system at one terminal,

$$\begin{bmatrix} u_1 \\ u_2 \end{bmatrix} = \begin{bmatrix} e_2^a \\ -e_1^b \end{bmatrix}, \quad \begin{bmatrix} y_1 \\ y_2 \end{bmatrix} = \begin{bmatrix} e_1^a \\ e_2^b \end{bmatrix}, \tag{18}$$

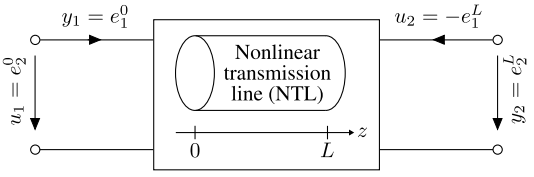

Fig. 1. In- and *collocated* outputs $(\boldsymbol{u}, \boldsymbol{y})$ of the considered nonlinear transmission systems.

[1]Greek letters are used for the distributed states and efforts, in order to distinguish from states and efforts of the discretized model in latin letters.

[2]From now on, the time dependency of the variables in the discretized model is dropped.

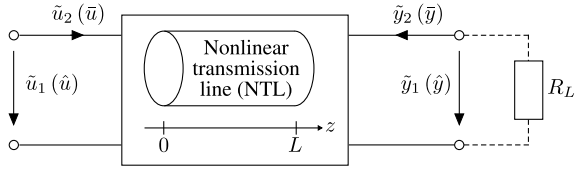

Fig. 2. Transmission system with non-collocated in- and outputs, possibly terminated by a resistive relation (dashed).

is depicted in Fig. 1. With an approximation of the distributed dissipative effects

$$r_i(\boldsymbol{x}) = (b-a)\rho_i(\frac{\boldsymbol{x}}{b-a}), \tag{19}$$

the port-Hamiltonian state representation of one discretized segment (superscript 1) of the transmission system is

$$\Sigma^1: \quad \begin{aligned} \dot{\boldsymbol{x}} &= (\boldsymbol{J}^1 - \boldsymbol{R}^1)\boldsymbol{e} + \boldsymbol{G}^1\boldsymbol{u} \\ \boldsymbol{y} &= (\boldsymbol{G}^1)^T\boldsymbol{e} + \boldsymbol{D}^1\boldsymbol{u}, \end{aligned} \tag{20}$$

where $\boldsymbol{x}$, $\boldsymbol{e}$, $\boldsymbol{u}$, $\boldsymbol{y} \in \mathbb{R}^2$, $\boldsymbol{e} = \nabla H^{ab}$, and

$$\begin{aligned} \boldsymbol{F}^1 = \boldsymbol{J}^1 - \boldsymbol{R}^1 &= \begin{bmatrix} -r_1(\boldsymbol{x}) & -2 \\ 2 & -r_2(\boldsymbol{x}) \end{bmatrix}, \\ \boldsymbol{G}^1 = \begin{bmatrix} \boldsymbol{g}_1^1 & \boldsymbol{g}_2^1 \end{bmatrix} = \begin{bmatrix} 2 & 0 \\ 0 & 2 \end{bmatrix}, &\quad \boldsymbol{D}^1 = \begin{bmatrix} 0 & 1 \\ -1 & 0 \end{bmatrix}. \end{aligned} \tag{21}$$

Remark 1: In the example of the electric transmission line, u_1 and y_1 are the voltage and current at the left terminal, u_2 and y_2 the current and voltage at the right end. Accordingly, this holds for other representatives of the system class. We call u_1 a voltage type input, and u_2 a current type input.

Remark 2: For a series connection of N segments, it can be shown that the error made by approximation (19) concerning the dissipative losses,

$$\int_a^b \rho_i(\boldsymbol{\zeta}(z))\beta_i^2(z)\,dz - r_i(\boldsymbol{x})e_i^2, \quad i = 1, 2, \tag{22}$$

tends to zero with an increasing number N of segments.

C. Recursive model construction

Connecting N discretized segments in series, each an approximation on the interval $[a_k, b_k]$, with $a_1 = 0$, $b_N = L$, as described in [4][3] based on the method from [1], the finite-dimensional port-Hamiltonian state representation $\{\boldsymbol{F}, \boldsymbol{G}, \boldsymbol{G}^T, \boldsymbol{D}\}$

$$\Sigma: \quad \begin{aligned} \dot{\boldsymbol{x}} &= \boldsymbol{F}\boldsymbol{e} + \boldsymbol{G}\boldsymbol{u} \\ \boldsymbol{y} &= \boldsymbol{G}^T\boldsymbol{e} + \boldsymbol{D}\boldsymbol{u} \end{aligned} \tag{23}$$

is obtained. Therein, $\boldsymbol{x}, \boldsymbol{e} \in \mathbb{R}^{2N}$, $\boldsymbol{u}, \boldsymbol{y} \in \mathbb{R}^2$, the efforts relate to the approximate energies through

$$\boldsymbol{e} = \nabla H(\boldsymbol{x}), \quad H = \sum_{k=1}^{N} H^{a_k b_k}, \tag{24}$$

[3]Therein, the indices of the in- and outputs are permuted.

TABLE I

NOTATION FOR THE DIFFERENT IN- AND OUTPUT CONSTELLATIONS

State representation	In- and outputs according to Figs. 1 and 2
Σ: $\{\boldsymbol{F}, \boldsymbol{G}, \boldsymbol{G}^T, \boldsymbol{D}\}$	Collocated in- and outputs $(\boldsymbol{u}, \boldsymbol{y})$
$\tilde{\Sigma}$: $\{\tilde{\boldsymbol{F}}, \tilde{\boldsymbol{G}}, \tilde{\boldsymbol{H}}, \tilde{\boldsymbol{D}}\}$	Non-collocated in- and outputs $(\tilde{\boldsymbol{u}}, \tilde{\boldsymbol{y}})$
$\hat{\Sigma}$: $\{\hat{\boldsymbol{F}}, \hat{\boldsymbol{g}}, \hat{\boldsymbol{h}}, \hat{d}\}$	SISO, voltage type in- and output $(\hat{u}, \hat{y})$
$\bar{\Sigma}$: $\{\bar{\boldsymbol{F}}, \bar{\boldsymbol{g}}, \bar{\boldsymbol{h}}, \bar{d}\}$	SISO, current type in- and output $(\bar{u}, \bar{y})$

TABLE II

RELATIONS BETWEEN IN- AND OUTPUTS IN THE DIFFERENT MODELS

		Σ	$\tilde{\Sigma}$	$\hat{\Sigma}$	$\bar{\Sigma}$
$z = 0$	e_2	u_1	$\tilde{u}_1$	$\hat{u}$	–
	e_1	y_1	$\tilde{u}_2$	–	$\bar{u}$
$z = L$	e_1	u_2	$\tilde{y}_2$	–	$\bar{y}$
	e_2	y_2	$\tilde{y}_1$	$\hat{y}$	–

and the matrices $\boldsymbol{F} = \boldsymbol{F}^N$, $\boldsymbol{G} = \boldsymbol{G}^N$, $\boldsymbol{D} = \boldsymbol{D}^N$ are constructed recursively, $K = 2, \ldots, N$, according to

$$\boldsymbol{F}^K = \begin{bmatrix} \boldsymbol{F}^{K-1} & -\boldsymbol{g}_2^{K-1}(\boldsymbol{g}_1^1)^T \\ \boldsymbol{g}_1^1(\boldsymbol{g}_2^{K-1})^T & \boldsymbol{F}^1 \end{bmatrix}, \tag{25}$$

$$\boldsymbol{g}_1^K = \begin{bmatrix} \boldsymbol{g}_1^1 \\ -\boldsymbol{g}_1^{K-1} \end{bmatrix}, \quad \boldsymbol{g}_2^K = \begin{bmatrix} -\boldsymbol{g}_2^{K-1} \\ \boldsymbol{g}_2^1 \end{bmatrix}, \tag{26}$$

$$\boldsymbol{D}^K = -\boldsymbol{D}^{K-1} = \begin{bmatrix} 0 & -(-1)^K \\ (-1)^K & 0 \end{bmatrix}. \tag{27}$$

Remark 3: The occurence of a feedthrough term in the discretized model is not surprising. From the definition of average efforts in Eq. (16), it is evident that a boundary effort at one terminal of a series interconnection of line segments can be expressed by all average efforts and the boundary effort at the opposite terminal.

D. Different state representations

Starting from the port-Hamiltonian state representation Σ in (23) and making use of the feedthrough term therein, different system models corresponding to different definitions of in- and outputs (collocated vs. non-collocated, MIMO, SISO) can be formulated. Table I shows the notation for the different cases which are illustrated in Figs. 1 and 2.

1) MIMO model, collocated in-/outputs: In the model Σ, (u_1, y_1) and (u_2, y_2) are pairs of collocated in- and outputs, each situated at one terminals of the system. From the structure of the equations and the positive definiteness[4] of the dissipation matrix $\boldsymbol{R} = -\frac{1}{2}(\boldsymbol{F} + \boldsymbol{F}^T)$ it follows that the energy balance equation $\dot{H} < \boldsymbol{y}^T\boldsymbol{u}$ holds. This discretized version approximates the energy balance (6) of the original infinite-dimensional model.

2) MIMO model, non-collocated in-/outputs: In $\tilde{\Sigma}$, the inputs $\tilde{\boldsymbol{u}}$ are defined as the boundary efforts at the left terminal, the outputs $\tilde{\boldsymbol{y}}$ accordingly as the efforts at the right one. The system matrices for this case are found by solving the first output equation of Σ for $u_2 = \tilde{y}_2$ and replacing the

[4]if both r_1 and r_2 are non-zero

expression in the differential equation:

$$\tilde{\boldsymbol{F}} = \boldsymbol{F} + (-1)^N \boldsymbol{g}_2 \boldsymbol{g}_1^T, \quad \tilde{\boldsymbol{G}} = \begin{bmatrix} \boldsymbol{g}_1 & -(-1)^N \boldsymbol{g}_2 \end{bmatrix}$$
$$\tilde{\boldsymbol{H}} = \begin{bmatrix} \boldsymbol{g}_2^T \\ (-1)^N \boldsymbol{g}_1^T \end{bmatrix}, \quad \tilde{\boldsymbol{D}} = (-1)^N \begin{bmatrix} 1 & 0 \\ 0 & -1 \end{bmatrix}. \tag{28}$$

If the system is terminated at the right end by a device which imposes a resistive relation between the efforts

$$e_2(L) = R_L e_1(L) \quad \Leftrightarrow \quad e_1(L) = \frac{1}{R_L} e_2(L), \tag{29}$$

like an ohmic load or a (state-dependent) outflow characteristics in the fluidic case, the number of independent outputs (and inputs) is reduced to one. Depending on which of the boundary efforts is assigned as the remaining input (e_2: voltage type, e_1: current type, inspired by the electrical transmission line), the following models can be derived:

3) SISO model, voltage type in-/outputs:

$$\hat{\boldsymbol{F}} = \boldsymbol{F} - \frac{1}{R_L} \boldsymbol{g}_2 \boldsymbol{g}_2^T, \quad \hat{\boldsymbol{g}} = \frac{-(-1)^N}{R_L} \boldsymbol{g}_2 + \boldsymbol{g}_1,$$
$$\hat{\boldsymbol{h}} = \boldsymbol{g}_2^T, \quad \hat{d} = (-1)^N. \tag{30}$$

4) SISO model, current type in-/outputs:

$$\bar{\boldsymbol{F}} = \boldsymbol{F} + (-1)^N (\boldsymbol{g}_2 \boldsymbol{g}_1^T - \boldsymbol{g}_1 \boldsymbol{g}_2^T) - R_L \boldsymbol{g}_1 \boldsymbol{g}_1^T,$$
$$\bar{\boldsymbol{g}} = -(-1)^N \boldsymbol{g}_2 + R_L \boldsymbol{g}_1,$$
$$\bar{\boldsymbol{h}} = (-1)^N \boldsymbol{g}_1^T, \quad \bar{d} = -(-1)^N. \tag{31}$$

Both SISO models $\hat{\Sigma}$ and $\bar{\Sigma}$ have a *non-collocated* pair of in- and output[5].

E. Inverse models

Permuting the roles of in- and outputs, the inverse discretized models[6] Σ', $\tilde{\Sigma}'$, $\hat{\Sigma}'$, $\bar{\Sigma}'$ are obtained. To express the system matrices, in the same manner as above, the corresponding output equation is solved for the input which then is replaced in the differential equation.

1) MIMO model, collocated, $\Sigma' : \{\boldsymbol{F}', \boldsymbol{G}', \boldsymbol{G}'^T, \boldsymbol{D}'\}$:

$$\boldsymbol{F}' = \boldsymbol{F} + \boldsymbol{G}\boldsymbol{D}\boldsymbol{G}^T, \quad \boldsymbol{G}' = -\boldsymbol{G}\boldsymbol{D}, \quad \boldsymbol{D}' = -\boldsymbol{D}. \tag{32}$$

2) MIMO model, non-collocated, $\tilde{\Sigma}' : \{\tilde{\boldsymbol{F}}', \tilde{\boldsymbol{G}}', \tilde{\boldsymbol{H}}', \tilde{\boldsymbol{D}}'\}$:

$$\tilde{\boldsymbol{F}}' = \boldsymbol{F} - (-1)^N \boldsymbol{g}_1 \boldsymbol{g}_2^T, \quad \tilde{\boldsymbol{G}}' = \begin{bmatrix} (-1)^N \boldsymbol{g}_1 & \boldsymbol{g}_2 \end{bmatrix}$$
$$\tilde{\boldsymbol{H}}' = \begin{bmatrix} -(-1)^N \boldsymbol{g}_2^T \\ \boldsymbol{g}_1^T \end{bmatrix}, \quad \tilde{\boldsymbol{D}}' = (-1)^N \begin{bmatrix} 1 & 0 \\ 0 & -1 \end{bmatrix}. \tag{33}$$

3) SISO model, voltage type, $\hat{\Sigma}' : \{\hat{\boldsymbol{F}}', \hat{\boldsymbol{g}}', \hat{\boldsymbol{h}}', \hat{\boldsymbol{D}}'\}$:

$$\hat{\boldsymbol{F}}' = \boldsymbol{F} - (-1)^N \boldsymbol{g}_1 \boldsymbol{g}_2^T, \quad \hat{\boldsymbol{g}}' = -\frac{1}{R} \boldsymbol{g}_2 + (-1)^N \boldsymbol{g}_1$$
$$\hat{\boldsymbol{h}}' = -(-1)^N \boldsymbol{g}_2^T, \quad \hat{d} = (-1)^N. \tag{34}$$

4) SISO model, current type, $\bar{\Sigma}' : \{\bar{\boldsymbol{F}}', \bar{\boldsymbol{g}}', \bar{\boldsymbol{h}}', \bar{\boldsymbol{D}}'\}$:

$$\bar{\boldsymbol{F}}' = \boldsymbol{F} - (-1)^N (\boldsymbol{g}_1 \boldsymbol{g}_2^T), \quad \bar{\boldsymbol{g}}' = \boldsymbol{g}_2 - (-1)^N R \boldsymbol{g}_1$$
$$\bar{\boldsymbol{h}}' = \boldsymbol{g}_1^T \quad \bar{d} = -(-1)^N. \tag{35}$$

[5]The collocated SISO case ist not considered here.

[6]The prime indicates the model inversion. In the inverse model the plant output appears as input in the differential equation.

TABLE III
DISSIPATION MATRICES FOR THE DIFFERENT MODELS

Models from Subsection II-D				Inverse Models, cf. II-E			
Σ	$\tilde{\Sigma}$	$\hat{\Sigma}$	$\bar{\Sigma}$	Σ'	$\tilde{\Sigma}'$	$\hat{\Sigma}'$	$\bar{\Sigma}'$
$\boldsymbol{R}$	$\tilde{\boldsymbol{R}}$	$\boldsymbol{R} + \frac{\boldsymbol{g}_2 \boldsymbol{g}_2^T}{R_L}$	$\boldsymbol{R} + R_L \boldsymbol{g}_1 \boldsymbol{g}_1$	$\boldsymbol{R}$	$\tilde{\boldsymbol{R}}$	$\tilde{\boldsymbol{R}}$	$\tilde{\boldsymbol{R}}$

III. PROPERTIES OF THE DISCRETIZED MODELS

In this section, we briefly discuss the properties of the obtained discretized models.

A. Stability

Assuming an energy function $H(\boldsymbol{x})$ which is bounded from below at the unforced equilibrium of a port-Hamiltonian system, asymptotic stability of this equilibrium is guaranteed if the dissipation matrix is positive definite. Taking the negative symmetric part of the $\boldsymbol{F}$-matrices, the dissipation matrices for the models presented in the preceding section follow according to Table III.

1) Collocated in-/outputs: The dissipation matrix in the collocated MIMO case for both the forward and inverse model Σ and Σ' is positive definite:

$$\boldsymbol{R} = -\frac{1}{2}(\boldsymbol{F} + \boldsymbol{F}^T) > 0, \qquad r_1, r_2 > 0. \tag{36}$$

This is not surprising as the inverse model is identically the dual model in the sense that only the roles of the boundary efforts (power variables) at each terminal are permuted.

2) Feedforward SISO models: In the cases $\hat{\Sigma}$, $\bar{\Sigma}$ of transmission systems terminated by a resistive relation, additional damping is injected into the system. Consequently, $\hat{\boldsymbol{R}}$ and $\bar{\boldsymbol{R}}$ remain positive definite.

3) Non-collocated in-/outputs: In the remaining four cases $\tilde{\Sigma}$, $\tilde{\Sigma}'$, $\hat{\Sigma}'$, $\bar{\Sigma}'$, including all inverse models with non-collocated in-/outputs, the dissipation matrix turns out to be

$$\tilde{\boldsymbol{R}} = \boldsymbol{R} - \frac{1}{2}(-1)^N (\boldsymbol{g}_1 \boldsymbol{g}_2^T + \boldsymbol{g}_2 \boldsymbol{g}_1^T). \tag{37}$$

Due to the possible indefiniteness of $\tilde{\boldsymbol{R}}$, the non-collocated cases are interesting. If $\tilde{\boldsymbol{R}}$ is positive definite, the inverse dynamics can be solved by a straightforward numerical integration. A bounded desired output trajectory $\tilde{\boldsymbol{y}}(t)$ (or $\hat{y}(t)$ or $\bar{y}(t)$) then results in a bounded state trajectory $\boldsymbol{x}(t)$ and a bounded input $\tilde{\boldsymbol{u}}(t)$ (or $\hat{u}(t)$ or $\bar{u}(t)$)[7]. If $\tilde{\boldsymbol{R}}$ is indefinite, the integration of the unstable inverse dynamics would produce unbounded state trajectories. In such a case the feedforward control problem corresponds to the dynamic inversion of non-minimumphase systems, which can be formulated as a two point boundary value problem [6], [10].

[7]This follows from Lemma 5.5 in [9]: Under a Lipschitz condition, input-to-state stability can be concluded from exponential stability with a radially unbounded Lyapunov function. (For simplicity, we also assume $H(\boldsymbol{x})$ to be radially unbounded.)

B. Definiteness condition

Based on the block structure of the dissipation matrix $\tilde{\boldsymbol{R}}$, a condition can be given for its positive definiteness:

Lemma 1: Assume identical dissipation coefficients $r_1, r_2 > 0$ in every segment of the discretized model. The dissipation matrix $\tilde{\boldsymbol{R}}$ of the inverse models $\tilde{\Sigma}'$, $\hat{\Sigma}'$, $\bar{\Sigma}'$ (and also the feedforward model $\tilde{\Sigma}$) is positive definite if and only if

$$r_1 r_2 > (2N)^2, \tag{38}$$

with N the number of segments of the discretized model.

Proof: $\tilde{\boldsymbol{R}} \in \mathbb{R}^{2N\times 2N}$ has the following structure:

$$\tilde{\boldsymbol{R}} = \begin{bmatrix} \boldsymbol{X} & \boldsymbol{Y} & -\boldsymbol{Y} & \boldsymbol{Y} & \dots \\ \boldsymbol{Y} & \boldsymbol{X} & \boldsymbol{Y} & -\boldsymbol{Y} & \dots \\ -\boldsymbol{Y} & \boldsymbol{Y} & \boldsymbol{X} & \boldsymbol{Y} & \\ \boldsymbol{Y} & -\boldsymbol{Y} & \boldsymbol{Y} & \boldsymbol{X} & \\ \vdots & \vdots & & & \ddots \end{bmatrix}, \tag{39}$$

where

$$\boldsymbol{X} = \begin{bmatrix} r_1 & -2 \\ -2 & r_2 \end{bmatrix}, \quad \boldsymbol{Y} = \begin{bmatrix} 0 & 2 \\ 2 & 0 \end{bmatrix}. \tag{40}$$

$\tilde{\boldsymbol{R}}$ can be transformed into a block triangular matrix with a zero matrix $\boldsymbol{O}_{N\times N}$ in the lower left corner by pairwise permuting rows and columns, which preserves the definiteness property. The definiteness of the transformed matrix can be checked with the help of the Schur decomposition. Doing this subsequently for models with $K = 1, \dots, N$ segments, condition (38) follows. □

Remark 4: Note that the bound for necessary dissipation increases with the number of segments N, while the values of r_i decrease when the segments become shorter. As a consequence, the condition can only be satisfied in heavily damped systems with a coarse spatial discretization. For weakly damped systems with a reasonably fine grid, the condition is violated in general.

C. Quality of the approximation

Despite the fact that the considered discretized models have vanishing relative degree, typical properties of the original PDE model are displayed by the discretization.

1) Convergence to exact solution: Figure 3 shows simulation results for the transmission line example from [1] with spline approximation and a uniform grid. The electric transmission line of length $L = e - 1$ with distributed inductance and capacitance $l(z)=1/(1+z)$, $c(z)=1/(1+z)$ is terminated with a resistance $R_L = 1$. The input voltage $\hat{u}(t) = v(0,t) = e_2(0,t) = \sin(t)\sigma(t)$ results in a delayed output $\hat{y}(t) = v(L,t) = e_2(L,t) = \sin(t-1)\sigma(t-1)$ for zero initial charge and flux densities $\psi(z,0)=x_1(z,0)=0$, $q(z,0) = x_2(z,0) = 0$. The zero relative degree causes an (unphysical) immediate reaction at the output. Its magnitude, however, is drastically reduced with an increasing number of grid points N such that the characteristic delay is reproduced quite well. The representation of the error $e(t)=v(L,t)-\hat{y}(t)$ in Fig. 3 documents the convergence of the approximation towards the exact solution for $t>1$.

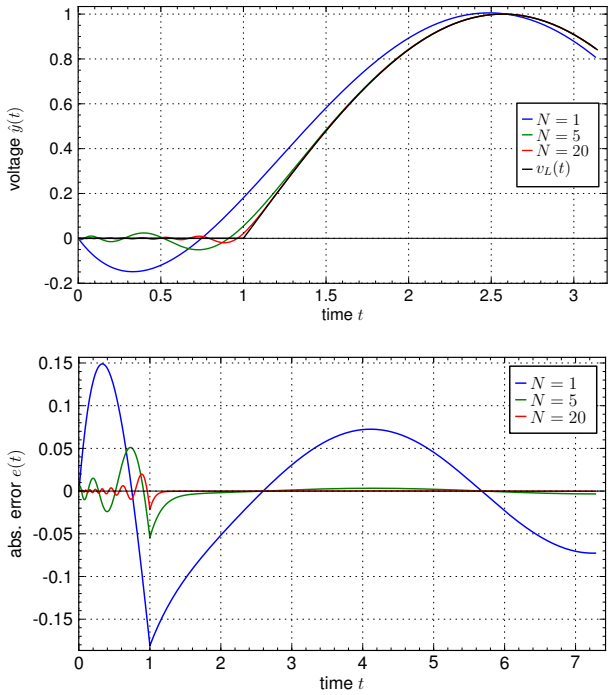

Fig. 3. Terminal voltage at the transmission line for $v_0(t) = \sin t$. Exact solution $v_L(t)$ vs. output $\hat{y}(t)$ of the discretized model with different numbers N of discretization intervals. Below: Error $e(t) = v_L(t) - \hat{y}(t)$.

2) Acausality in the non-collocated MIMO model: The dissipation matrix $\tilde{\boldsymbol{R}}$ in the non-collocated MIMO model $\tilde{\Sigma}$ (and its inverse $\tilde{\Sigma}'$) has one negative and one positive eigenvalue when condition (38) is violated. In this case, the state transition matrix for linear systems (or the nonlinear transition operator for the nonlinear case, see [10]) contains causal and acausal terms. This is in full accordance with the properties of the PDE model. Consider as an example the analytic solutions of the Telegrapher's equations with dissipation, see Eq. (10) in [11]. Therein, the computation of currents and voltages at one terminal requires future values of these quantities at the opposite end.

IV. FEEDFORWARD CONTROL

In the following, desired s-shaped transient trajectories $\tilde{y}_i(t)$, $i = 1, 2$ are considered, connecting two admissible equilibria $\boldsymbol{x}_A^*$ and $\boldsymbol{x}_B^*$ of the discretized system $\tilde{\Sigma}$ with non-collocated in-/outputs. In Fig. 4, such a trajectory is depicted with sufficiently long constant continuations before and after to account for pre- and postactuation periods. These will be necessary due to the acausality of the transition matrix/operator. The solution procedure sketched below reflects the approach for the stable inversion of non-minimum phase systems described in [6], [10][8].

To determine the feedforward control, the modularity of the considered discretized port-Hamiltonian models is exploited. Instead of seeking a solution based on the complete

[8]Observe that $\tilde{\Sigma}$ and $\tilde{\Sigma}'$ describe the system in an identical way, only with the role of the terminals interchanged. Hence, if $\tilde{\Sigma}$ (or $\tilde{\Sigma}'$) is unstable, it is also non-minimumphase, and its dynamic inversion can be tackled by the mentioned approach.

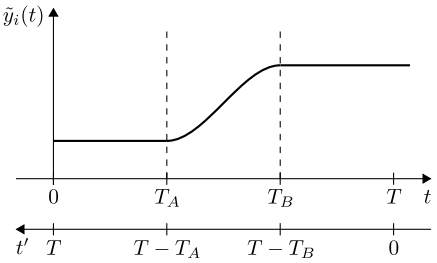

Fig. 4. Shape of the transient output trajectories with pre- and post-actuation intervals and inverse timescale.

model of an N-segment discretized system, the integration of the inverse system is executed segment-wise. This reduces the complexity of the subproblems and yields a conceptually simple computational scheme. The second order inverse state representation of a single segment with non-collocated in- and outputs (the i-th segment in a series interconnection) is given by

$$\tilde{\Sigma}_i': \quad \begin{aligned} \dot{\boldsymbol{x}}_i &= \tilde{\boldsymbol{F}}_i' \boldsymbol{e}_i + \tilde{\boldsymbol{G}}_i' \tilde{\boldsymbol{y}}_i \\ \tilde{\boldsymbol{u}}_i &= \tilde{\boldsymbol{H}}_i' \boldsymbol{e}_i + \tilde{\boldsymbol{D}}_i' \tilde{\boldsymbol{y}}_i, \end{aligned} \tag{41}$$

with $\boldsymbol{e}_i = \nabla H_i(\boldsymbol{x}_i)$ and

$$\tilde{\boldsymbol{F}}_i' = \begin{bmatrix} -r_{1,i} & 2 \\ 2 & -r_{2,i} \end{bmatrix}, \qquad \tilde{\boldsymbol{G}}_i' = \begin{bmatrix} -2 & 0 \\ 0 & 2 \end{bmatrix},$$
$$\tilde{\boldsymbol{H}}_i' = \begin{bmatrix} 0 & 2 \\ 2 & 0 \end{bmatrix}, \qquad \tilde{\boldsymbol{D}}_i' = \begin{bmatrix} -1 & 0 \\ 0 & 1 \end{bmatrix}.$$

For linear systems, the solution procedure, which involves integrations along the stable and unstable manifolds, forward and backward in time [6], is straightforward, as described below. In the nonlinear setting, which will be discussed rightafter, numerical procedures as a Picard-like iteration [10] are necessary.

A. Quadratic Hamiltonian

A quadratic Hamiltonian (for one segment) $H_i(\boldsymbol{x}_i) = \frac{1}{2}\boldsymbol{x}_i^T \boldsymbol{Q}_i \boldsymbol{x}_i$, $\boldsymbol{Q}_i = \boldsymbol{Q}_i^T > 0$ is assumed, as well as constant dissipation terms $r_{1,i}, r_{2,i} > 0$. The inverse state representation $\tilde{\Sigma}_i'$ of the i-th segment can then be written in the standard form of a linear time-invariant system ($\boldsymbol{x}_i, \tilde{\boldsymbol{y}}_i, \tilde{\boldsymbol{u}}_i \in \mathbb{R}^2$)

$$\begin{aligned} \dot{\boldsymbol{x}}_i &= \boldsymbol{A}_i \boldsymbol{x}_i + \boldsymbol{B}_i \tilde{\boldsymbol{y}}_i \\ \tilde{\boldsymbol{u}}_i &= \boldsymbol{C}_i \boldsymbol{x}_i + \boldsymbol{D}_i \tilde{\boldsymbol{y}}_i \end{aligned} \tag{42}$$

with $\boldsymbol{A}_i = \tilde{\boldsymbol{F}}_i' \boldsymbol{Q}_i$, $\boldsymbol{B}_i = \tilde{\boldsymbol{G}}_i'$, $\boldsymbol{C}_i = \tilde{\boldsymbol{H}}_i' \boldsymbol{Q}_i$, $\boldsymbol{D}_i = \tilde{\boldsymbol{D}}_i'$. Assuming that $\boldsymbol{A}_i$ has one negative and one positive eigenvalue, λ_i^- and λ_i^+,[9] a modal transformation $\boldsymbol{x}_i = \boldsymbol{V}_i \boldsymbol{\xi}_i$, where $\boldsymbol{V}_i$ is composed of the right hand eigenvectors of $\boldsymbol{A}_i$, brings the state differential equation into the form

$$\begin{aligned} \dot{\xi}_{i,1} &= \lambda_i^- \xi_{i,1} + \nu_{i,1} \\ \dot{\xi}_{i,2} &= \lambda_i^+ \xi_{i,2} + \nu_{i,2}. \end{aligned} \tag{43}$$

The transformed inputs $\nu_{i,j} = \boldsymbol{w}_{i,j}^T \boldsymbol{B} \tilde{\boldsymbol{y}}_i$, $j = 1, 2$ are computed from the desired output trajectory $\tilde{\boldsymbol{y}}_i$ and the left hand eigenvectors $\boldsymbol{w}_{i,j}^T$ of the i-th segment. While the differential equation associated with the stable mode λ_i^- can be integrated in forward time to determine the trajectory of $\xi_{i,1}$, the second state $\xi_{i,2}$ follows from an integration in reverse time. With the time transformation $t' = T - t$ and the definition of the reverse time signals $\nu_{i,2}'(t') = \nu_{i,2}(T - t')$ and $\xi_{i,2}'(t') = \xi_{i,2}(T - t')$, the unstable differential equation is transformed into the stable one

$$\dot{\xi}_{i,2}' = -\lambda_i^+ \xi_{i,2}' - \nu_{i,2}'. \tag{44}$$

After a backtransformation $\xi_{i,2}(t) = \xi_{i,2}'(T - t)$ the input trajectory $\tilde{\boldsymbol{u}}_i$ to achieve the output $\tilde{\boldsymbol{y}}_i$ at the opposite terminal of the i-th segment is computed from

$$\tilde{\boldsymbol{u}}_i = \boldsymbol{C}_i \boldsymbol{V} \tilde{\boldsymbol{\xi}}_i + \boldsymbol{D}_i \tilde{\boldsymbol{y}}_i. \tag{45}$$

Starting with the desired output at the terminal of the N-segment transmission line $\tilde{\boldsymbol{y}} = \tilde{\boldsymbol{y}}_N$ and setting $\tilde{\boldsymbol{y}}_{k-1} = \tilde{\boldsymbol{u}}_k$ after each step, the input $\tilde{\boldsymbol{u}} = \tilde{\boldsymbol{u}}_1$ at the opposite terminal can be iteratively determined.

B. Nonquadratic energy function

If the energies $H_i(\boldsymbol{x}_i)$ are nonquadratic, things are more delicate. In order to obtain a state representation like (43), an invertible, smooth coordinate transformation (diffeomorphism) $\boldsymbol{\xi}_i = \boldsymbol{t}_i(\boldsymbol{x}_i)$, $\boldsymbol{x}_i = \boldsymbol{t}_i^{-1}(\boldsymbol{\xi}_i)$ is required such that the nonlinear state differential equation for one segment

$$\dot{\boldsymbol{x}}_i = \boldsymbol{f}_i(\boldsymbol{x}_i) + \boldsymbol{B}_i \tilde{\boldsymbol{y}}_i \tag{46}$$

becomes

$$\begin{aligned} \dot{\xi}_{i,1} &= \lambda_i^- \xi_{i,1} + \nu_{i,1}(\boldsymbol{\xi}_i) \\ \dot{\xi}_{i,2} &= \lambda_i^+ \xi_{i,2} + \nu_{i,2}(\boldsymbol{\xi}_i). \end{aligned} \tag{47}$$

The coordinate functions $t_i(\boldsymbol{x})$ in this case must satisfy the quasilinear partial differential equations

$$\frac{\partial t_{i,j}(\boldsymbol{x}_i)}{\partial \boldsymbol{x}_i} \boldsymbol{f}_i(\boldsymbol{x}_i) = \lambda_i^{-/+} t_{i,j}(\boldsymbol{x}_i), \qquad j = 1, 2, \tag{48}$$

and the new input functions become

$$\nu_{i,j}(\boldsymbol{\xi}_i) = \frac{\partial t_{i,j}}{\partial \boldsymbol{x}_i} \circ \boldsymbol{t}_i^{-1}(\boldsymbol{\xi}_i) \cdot \boldsymbol{B}_i \tilde{\boldsymbol{y}}_i. \tag{49}$$

Note that the latter depend on the state $\boldsymbol{\xi}_i$, hence (47) is not a system of decoupled differential equations anymore, see the remark at the end of the section. However, the initial and final values for the states trajectory are known. Another possibility is a transformation to a more general triangular form and subsequent integration in both directions.

In case that a state trajectory $\boldsymbol{\xi}_i$ can be computed from the transformed state differential equation, involving some forward and backward integration, the input function to track the output $\tilde{\boldsymbol{y}}_i$ follows from

$$\tilde{\boldsymbol{u}}_i = \boldsymbol{h}_i(\boldsymbol{t}_i^{-1}(\boldsymbol{\xi}_i)) + \boldsymbol{D}_i \tilde{\boldsymbol{y}}_i. \tag{50}$$

Remark 5: The procedure for the nonlinear setting is a sketch which is directly inspired by the linear case. In order to derive a feasible numerical scheme for segment-wise

[9] This is certainly the case when the dissipation condition (38) is violated and $\boldsymbol{Q}_i$ is diagonal.

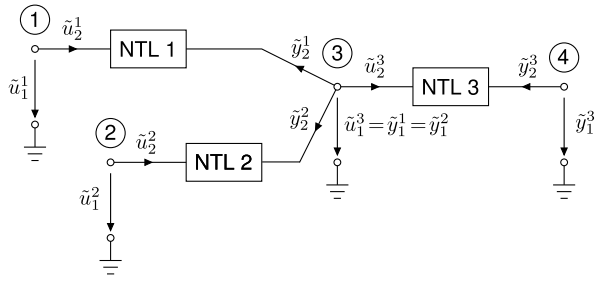

Fig. 5. Simplest star-shaped network of nonlinear transmission lines (NTL) as an electric equivalent circuit

feedforward control based on the above approach, some work remains to be done:

- The numerical solution of the quasilinear PDEs for the coordinate transformation (48) with the method of characteristics (or correspondingly for a transformation to triangular form).
- A numerical iteration scheme to solve the transformed differential equations (47) in order to determine the state trajectories.
- Comparison with existing numerical approaches, e. g. the Picard-like iteration in [10] or as presented in [11]. Therein, the feedforward control problem for the shallow water equation is solved based on the diagonalized PDEs. To obtain the solution, in each iteration step the characteristics are determined numerically, and an integration along them is performed.

V. APPLICATION TO NONLINEAR TRANSMISSION NETWORKS

The segment-wise method presented in the previous section for linear discretized systems, and sketched for the nonlinear case, can be applied to the feedforward control problem within networks of transmission systems.

In [7] the following feedforward problem is posed: In a HVDC network, current and voltage at a certain node have to be tracked / controlled by appropriate trajectories of current or voltage of the remaining converter nodes. Thereby, the network structure introduces additional degrees of freedom, so-called current allocation parameters. The solution presented in [7] employs the known analytic solutions of the linear line equations (for a single line). The ideas described in our paper can be used to solve the corresponding feedforward control problem in networks of *nonlinear* transmission lines (NTL), using the same rationale, replacing the analytic solution of the linear line equations by a numerical scheme.

VI. CONCLUSIONS AND OPEN QUESTIONS

The contribution of this paper is a discussion on the feedforward control problem for nonlinear transmission systems, based on the models obtained from structure preserving port-Hamiltonian discretization. Due to the occurence of a feedthrough term it is easy to formulate the inverse model for non-collocated pairs of in- and outputs. The inverse dynamics has to be integrated numerically in order to obtain the input trajectory. In general, the dissipation condition proposed in Section III is violated, and hence, the system to integrate is unstable. With the ideas from the dynamic inversion of non-minimum phase systems, i. e. a forward and backward integration along stable and unstable manifolds, a modular solution for the feedforward control problem can be sketched, as presented in Section IV. This solution is a computational building block to be used in the operation of networks of nonlinear transmission lines, e. g. to realize transients between two steady states.

Quite some work remains to be done: The issues to implement the modular dynamic inversion procedure for the nonlinear case, mentioned in Remark 5, need to be addressed. The procedure presented here has to be tested in simulations and compared with existing results for feedforward control of hyperbolic distributed parameter systems, like [11], where the methods of characteristics is used to derive feedforward controllers for an open channel flow. The comparison with the analytical solution for the linear Telegrapher's equations will provide qualitative information on the order of the discretized model in order to obtain reasonable results.

Another interesting issue is to apply a different structure-preserving discretization scheme, leading to different properties of the resulting models, like full relative degree. In such a case, the flatness-based approach seems appropriate. The difficulty then is to find the differential parametrizations of states and inputs in the general case of nonlinear, fully damped port-Hamiltonian models.

ACKNOWLEDGMENT

The first author thanks Jacquelien Scherpen and Arjan van der Schaft for the fruitful discussions during his stay in Groningen.

REFERENCES

[1] G. Golo, V. Talasila, A. van der Schaft, and B. Maschke, "Hamiltonian discretization of boundary control systems," *Automatica*, vol. 40, no. 5, pp. 757–771, 2004.
[2] A. J. van der Schaft and B. M. Maschke, "Hamiltonian formulation of distributed-parameter systems with boundary energy flow," *Journal of Geometry and Physics*, vol. 42, no. 1, pp. 166–194, 2002.
[3] B. Hamroun, L. Lefevre, and E. Mendes, "Port-based modelling for open channel irrigation systems," in *Proc. Int. Conf. Water Resources, Hydraulics & Hydrology, Portoroz, Slovenia*, 2006, pp. 41–46.
[4] P. Kotyczka, "Discretized models for networks of distributed parameter port-Hamiltonian systems," in *Multidimensional Systems (nDS), 2013. Proceedings of the 8th International Workshop on*, 2013, pp. 63–67.
[5] K. Graichen, V. Hagenmeyer, and M. Zeitz, "A new approach to inversion-based feedforward control design for nonlinear systems," *Automatica*, vol. 41, pp. 2033–2041, 2005.
[6] D. Chen and B. Paden, "Stable inversion of nonlinear non-minimum phase systems," *Int. J. Control*, vol. 64, pp. 81–97, 1996.
[7] C. Schmuck, F. Woittennek, A. Gensior, and J. Rudolph, "Feedforward control of an HVDC power transmission network," *IEEE Trans. Contr. Syst. Tech.*, vol. 22, no. 2, pp. 597–606, 2014.
[8] A. J. van der Schaft, "Port-Hamiltonian systems: an introductory survey," in *Proc. Int. Congress of Mathematicians, Madrid*, 2006, pp. 1339–1365.
[9] H. K. Khalil, *Nonlinear Systems*, 2nd ed. Prentice-Hall, 1996.
[10] S. Devasia, D. Chen, and B. Paden, "Nonlinear inversion-based output tracking," *Automatic Control, IEEE Transactions on*, vol. 41, no. 7, pp. 930–942, 1996.
[11] T. Knüppel, F. Woittennek, and J. Rudolph, "Flatness-based trajectory planning for the shallow water equations," in *Decision and Control (CDC), 2010 49th IEEE Conference on*, 2010, pp. 2960–2965.